EUMETSAT OSI SAF

Determining Bias Correction and Covariance Parameters for Optimal Estimation of Sea Surface Temperature

Visiting Scientist Report

Reference OSI_VS18_03

Version : v1.0

Date : 1/2/2019

Prof Christopher Merchant

Department of Meteorology, University of Reading, UK

National Centre for Earth Observation, UK

Document Change record

Document version	Software version	Date	Author	Change description
			CH	

Table of contents

1. Executive Summary

Optimal estimation SST is currently undertaken with error covariance matrix assumptions based on heuristics and expert assumptions. Incorrect specification causes the “optimal” retrievals in fact to be sub-optimal. This study demonstrates new methods to estimate appropriate parameters for OE, adapting ideas from Kalman filtering and Desroziers diagnostics in data assimilation. These methods are shown to improve SST error statistics and retrieval sensitivity. Additional insights into the nature of prior and forward model biases, including the degree of cross-channel simulation-error covariance and angular dependencies, are further obtained.

Disclaimer

2. Introduction

Optimal estimation (Rodgers, 2001) has been applied to the remote sensing of sea surface temperature (SST) from space in several studies (e.g., Merchant et al., 2008; Merchant et al.,2009), and has been widely applied to the retrieval of cloud properties, aerosol loadings and gas concentrations in the atmosphere.

Despite this heritage, use of optimal estimation is not without problems. OE assumes access to a forward model that can simulate observations with known uncertainty and zero-mean bias. In practice, the accuracies of the calibration of satellite sensors and of radiative transfer simulation through the atmosphere are not sufficient to guarantee that bias of the forward model relative to observations are negligible. Specific criticism of the application of OE to SST (Koner et al., 2015) has centred on the problem of determining appropriate error covariance parameters that are used in OE to give optimal weights to prior information and new observations when determining the solution. These parameters have typically been estimated from knowledge of satellite sensor specifications, the degree to which radiative transfer models disagree, and validation of information used as prior knowledge. Expert judgement is involved, and it is desirable to put estimation of error covariance parameters on a more objective footing.

In this paper, we demonstrate methods addressing both problems (estimating bias corrections and estimating error covariance matrices) in the context of retrieval of SST. The methods require anchoring to a reference, and for this a dataset of matches between satellite and in situ measurements of SST is used. The essence of the bias correction method is to retrieve the necessary parameters progressively from many satellite-in-situ matches, thereby extending OE to be “bias-aware” [Dee et al., 2005]. This method draws on the well-known technique of Kalman filtering, although not here applied sequentially in time. The essence of the error covariance method is to interrogate the pre- and post-retrieval residuals between the forward model and observations, using formulations derived by Desroziers et al. [2005] for application in data assimilation. The diagnostic has been used in the context of numerical weather prediction to estimate uncertainties for a variety of atmospheric observations including those from IASI and SEVIRI (Stewart et al 2013, Waller et al 2016a, Waller et al 2016b, Cordoba et al 2016). The use of improved observation error statistics in operational assimilation has resulted in improved analyses and forecast skill (Weston et al 2014, Bormann et al 2016, and Campbell et al 2017).

The next section of this paper expands upon this short introduction: sea surface temperature by optimal estimation is placed in the context of alternative retrieval methods, the equations of OE are presented as formulated for SST retrieval, and criticisms of the approach further explained. Section 3 describes the particularities of the data used in this study, and the operational context for the work. Section 4 presents the method of estimating bias correction, and section 5 the method of estimating error covariance matrices. The results are shown in section 6 in comparison with other options for SST retrieval (regression-based coefficients and modified total least squares). The paper concludes with a discussion of the practical importance of what has been presented.

3. Sea Surface Temperature Retrieval

Sea surface temperature (SST) retrieval methods first linearise the inverse problem by using brightness temperatures instead of radiances. Having taking this step, SST retrievals generally take the form of weighted linear combinations of two or more BTs. Different “algorithms” are different ways of determining the weights by means that are informed by the retrieval context to different degrees.

The method addressed here is optimal estimation using a reduced state vector of SST and total column water vapour [Merchant et al., 2008].

The equation for this optimal estimate are:

$$\hat{\boldsymbol{z}} = \boldsymbol{z}_a + (\boldsymbol{K}^{\mathrm{T}}\boldsymbol{S}_\epsilon^{-1}\boldsymbol{K} + \boldsymbol{S}_a^{-1})^{-1}\boldsymbol{K}^{\mathrm{T}}\boldsymbol{S}_\epsilon^{-1}(\boldsymbol{y} - \boldsymbol{F}) \qquad \text{Eq. 1}$$

$$\boldsymbol{z}_a = \begin{bmatrix} x_a \\ w_a \end{bmatrix}$$

$$\boldsymbol{F} = \boldsymbol{F}(\boldsymbol{x}_a)$$

$$\boldsymbol{K} = \frac{\partial \boldsymbol{F}}{\partial \boldsymbol{z}}|_{\boldsymbol{z}_a}$$

where, in this specific case: the observation vector contains the observations of three thermal channels of SEVIRI, $\boldsymbol{y} = \begin{bmatrix} y_{8.7} \\ y_{10.8} \\ y_{12.0} \end{bmatrix}$, where the subscript indicates the nominal central wavelength of the channel; the forward model, $\boldsymbol{F}$, used to simulate these channels is RTTOV v11.1; the prior state, $\boldsymbol{x}_a$, is (1) ECMWF forecast atmosphere (2) most recent OSTIA analysis SST (designated x_a); the prior TCWV, w_a, is the vertical integral of the water vapour density profile; $\frac{\partial \boldsymbol{F}}{\partial w}$ is evaluated by assuming that the water vapour density changes by the same fraction at all levels.

The present study changes none of the above formulation, but does address the error covariance assumptions. The initial formulation (based on Merchant et al., 2009) is that the observation error covariance (prior to recalculation) is modelled in terms of estimates of sensor noise an RTTOV uncertainty that increases at higher satellite zenith angles (in units K^2):

$$\boldsymbol{S}_\epsilon = \begin{bmatrix} 0.11^2 & 0 & 0 \\ 0 & 0.11^2 & 0 \\ 0 & 0 & 0.15^2 \end{bmatrix} + \begin{bmatrix} 0.15^2 s^2 & 0 & 0 \\ 0 & 0.15^2 s^2 & 0 \\ 0 & 0 & 0.15^2 s^2 \end{bmatrix} \qquad \text{Eq. 2}$$

where $s = \sec(\theta)$ (atmospheric path length of observation relative to nadir view). The off-diagonal terms are zero, although error correlation is expected, as discussed further below.

The initial formulation for the prior error covariance is that SST uncertainty is constant, whereas the uncertainty in TCWV itself depends on TCWV:

Eq. 3

$$\boldsymbol{S}_a = \begin{bmatrix} u_x^2 & 0 \\ 0 & u_w^2 \end{bmatrix}$$

$$u_x = \begin{cases} 0.2\ \mathrm{K}, & \text{drifting buoy} \\ 1.6\ \mathrm{K}, & \text{used for retrieval} \end{cases}$$

$$u_w = 0.5 w_a (0.1 + \frac{7.5 - w_a}{15})$$

for w_a in g cm^{-2}. The uncertainty of 1.6 K used for retrieval is large for reasons discussed in Merchant et al., 2009. Under diurnal warming conditions (rare but important) the observed skin SST will deviate from the prior (e.g., the OSTIA daily analysis product) by up to +5 K. A large value means the retrieval is able to capture these events

4. Data Used

In this study, we use a dataset of observations from SEVIRI matched to drifting buoy observations. The SEVIRI sensor in question is operational on the platform Meteosat-09, which was launched in December 2005. The buoy observations are within the field of view of the SEVIRI pixel and within 30 minutes of the pixel acquisition time. The SEVIRI cloud screening, quality flagging (see below) and matching are done within the systems of the Ocean and Sea-Ice Satellite Applications Facility used to produce the SEVIRI SST data record OSI-250 (http://www.osi-saf.org/?q=content/msgseviri-sea-surface-temperature-data-record).

Two years of data are exploited: data from the year 2011 are used as a training set from which parameters are derived, and the quoted results are for the application of those parameters to data from the year 2012. There is no particular significance of these years, other than match-up data (MD) being accessible with an augmented set of contextual information (see below).

There are 179,992 satellite-buoy matches in the 2011 (training) MD, and 165,574 in the 2012 (test) MD. The distribution of matches in 2011 is illustrated in Figure 1. In 2012 they are similarly distributed. The information in the dataset includes: the satellite (brightness temperature, BT) and drifting buoy (SST) measurements; a quality level (QL), derived in the OSI SAF processing system from a number of considerations such as proximity to flagged clouds; a numerical weather prediction (NWP) forecast of the atmospheric temperature and humidity profiles, needed as input for radiative transfer simulation of SEVIRI BTs; an operational estimate of the simulation bias relative to the satellite observations, estimated on timescales of 3 days on spatial scales of order 5 degrees from averages of simulation minus observation differences in night-time data; spatio-temporal geolocation information, such as satellite zenith angle; and the value of SST from the operational SST analysis, OSTIA, for the location and day. All the above fields are available within the operational processing system and can be exploited in near-real time.

Since the recommended OSI-SAF SSTs comprise those from pixels with QL 4 and 5, only those pixels are included in the MD. Quality control flags for identifying outlier drifting-buoy temperatures have been applied, along with an additional filter for those temperatures relative to OSTIA, in which matches were rejected where the differences exceeds 2 K, which being around ten times the expected uncertainty in drifting buoy SST (e.g., Lean and Saunders, 2013).

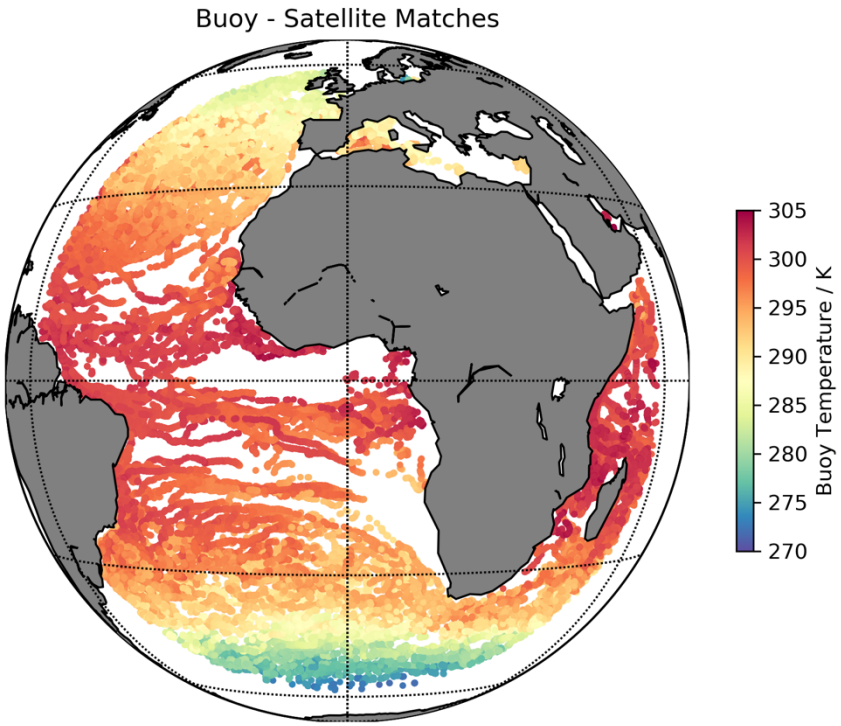

Figure 1. Distribution of satellite-buoy matches used in this study. The locations shown are for 2011, and other years are similar. Matched locations are coloured with the measured buoy sea surface temperature.

The radiative transfer model, RTTOV v11.2, was run for each match on the NWP profiles for the SEVIRI observation geometry, assuming cloud-free no-aerosol conditions. The SST used in the simulation was the drifting buoy SST minus a static adjustment for the ocean thermal skin effect of 0.17 K. The ocean skin effect is variable (e.g., Minnett et al., 2011; Wong and Minnett, 2018), and for the present purpose, this adjustment is intended to correct for the mean skin effect to within an uncertainty of order 0.1 K.

5. Methods: Derivation and Application

5.1. Overview

This paper describes methods for three steps of parameter estimation to improve optimal estimation results for SST. These steps are residual bias correction, simulation-observation error covariance estimation, and prior error covariance estimation. The parameters estimated in each step are contained in a vector of bias correction parameters, $\boldsymbol{\beta}$, and two covariance matrices, $\boldsymbol{S}_\epsilon$ and $\boldsymbol{S}_a$, respectively. The steps are undertaken sequentially, but are not independent, in that the current evaluation of each parameter set influences the evaluation of the others. The optimisation of the parameters is therefore iterative, and is sequenced as in Figure 2. This methods section presents each step, in turn: initialisation, bias correction estimation, simulation-observation error covariance estimation, prior error covariance estimation and testing for convergence.

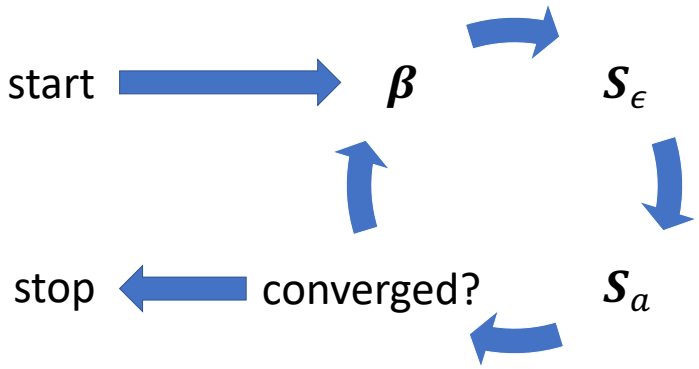

Figure 2. The sequence of estimation of three sets of parameters for optimal estimation. For symbols, see the main text.

5.2. Initialisation

The OSI-SAF ran an optimal estimation retrieval as an experimental processing chain on matches for 2011 and 2012. The initial estimates of the OE parameters are the values of the parameters in that experimental chain. These have been specified over a period of time based on case studies, expert judgement, understanding of SEVIRI sensor characteristics, etc.

The parameters $\boldsymbol{\beta}$ consist of a single bias parameter per channel, such that $\boldsymbol{\beta} = \begin{bmatrix} \beta_{8.7} \\ \beta_{10.8} \\ \beta_{12.0} \end{bmatrix}$, using a notation analogous to that introduced above for $\boldsymbol{y}$. While the biases are likely to be complex and variable, it is assumed in this study that much of that variability is captured by the bias adjustment procedure of the OSI SAF processing. Nonetheless, the SSTs from the experimental processing chain are biased overall, the absolute mean difference in validation exceeding a nominal target of 0.1 K. (The validation statistics are presented below in section §6.2, in the context of the improvements achieved by the present study.) The SST biases are found to be different between QL 4 and QL 5, therefore $\boldsymbol{\beta}$ is estimated separately for each QL. However, the initial estimates for bias is 0 K for every channel at both QLs.

The initial model for the observation-simulation error covariance is given by Eq. 4,

$$\boldsymbol{S}_\epsilon = \begin{bmatrix} {u_{8.7}^o}^2 & 0 & 0 \\ 0 & {u_{10.8}^o}^2 & 0 \\ 0 & 0 & {u_{12.0}^o}^2 \end{bmatrix} + \begin{bmatrix} {u_{8.7}^s}^2 s^2 & 0 & 0 \\ 0 & {u_{10.8}^s}^2 s^2 & 0 \\ 0 & 0 & {u_{12.0}^s}^2 s^2 \end{bmatrix} \quad \text{Eq. 4}$$

where: $s = \sec(\theta)$, where θ is the satellite zenith angle, and s is therefore the length of the path of the ray from the surface to the satellite through the atmosphere relative to a nadir ray (hereafter referred to as the 'path'); u_λ^o is the uncertainty of observation for the channel centred on λ μm; and u_λ^s is the corresponding simulation uncertainty. The numerical values are given in Table 1. Eq. 4 embodies some prior expectation about the error-covariance structure and has some limitations. The diagonal form of the observation error covariance expresses the expectation that this is dominated by radiometric noise, which his independent between the BTs of different channels. The values of the noise levels were estimated in Merchant et al (2013). The simulation uncertainties are modelled as being proportional to the path, expressing the understanding that the parameterisation of the RTTOV model is more accurate for a nadir path than at high zenith angles. A limitation of this formulation is that the simulation errors are assumed to be uncorrelated between channels. Since the parameterisation of the RTTOV model has the same form in all these channels, in fact it is reasonable to expect that the simulation errors have some degree of correlation.

Table 1. Initial assumptions about observation-simulation uncertainties.

	Observation Uncertainty / K			Nadir simulation Uncertainty / K		
Channel	8.7	10.8	12.0	8.7	10.8	12.0
Estimate	0.11	0.11	0.15	0.15	0.15	0.15

The initial model for the prior error covariance is also diagonal:

$$\boldsymbol{S}_a = \begin{bmatrix} u_x^2 & 0 \\ 0 & u_w^2 \end{bmatrix}; u_w = aw_a + bw_a^2 \quad \text{Eq. 5}$$

with the values $u_x = 1.6$ K, $a = \frac{3}{10}$ and $b = \frac{1}{30}$, for the prior total column water vapour, w_a. The value of 1.6 K exceeds the uncertainty in OSTIA or drifting buoys considerably, and will not be used in this study: it was chosen in the context of ensuring strong sensitivity to SST in the OE retrieval. Here, a realistic estimate for drifting buoy uncertainty, 0.2 K, is used initially. It is reasonable to expect that the SST and TCWV errors are uncorrelated.

5.3. Estimating S-O bias

The parameters $\boldsymbol{\beta}$ are here defined such that adding them to the forward model corrects for bias. The concept for estimating the parameters is essentially to retrieve them, adding the parameters to the state vector. The is achieved iteratively, progressively refining the estimates of the parameters over many retrievals. The anchoring for the bias estimates is provided by the drifting buoy SSTs, which, on average, are assumed (after correcting for the skin effect) to give a well-calibrated reference. The SST prior for each retrieval is therefore the matched drifting buoy SST. The iterative approach is related to Kalman filtering (Rodgers, 2001) which may be used sequentially to estimate both the state and parameters of a model, but here there is no spatio-temporal continuity and there are some other differences (explained below).

The mathematical formulation of the i^{th} retrieval is:

$$\tilde{\boldsymbol{z}}_i = \tilde{\boldsymbol{z}}_a + \left(\tilde{\boldsymbol{K}}^{\mathrm{T}}\boldsymbol{S}_\epsilon^{-1}\tilde{\boldsymbol{K}} + \tilde{\boldsymbol{S}}^{-1}\right)^{-1}\tilde{\boldsymbol{K}}^{\mathrm{T}}\boldsymbol{S}_\epsilon^{-1}(\boldsymbol{y} - \boldsymbol{\beta}_{i-1} - \boldsymbol{F}) \qquad \text{Eq. 6}$$

$$\tilde{\boldsymbol{z}}_a = \begin{bmatrix}\boldsymbol{z}_a \\ \boldsymbol{\beta}_{i-1}\end{bmatrix} = [x_b \quad w_a \quad \beta_{8.7,i-1} \quad \beta_{10.8,i-1} \quad \beta_{12.0,i-1}]^{\mathrm{T}}$$

$$\tilde{\boldsymbol{K}} = \begin{bmatrix}\frac{\partial \boldsymbol{F}}{\partial \boldsymbol{z}}|_{\boldsymbol{z}_a} & \boldsymbol{I}_3\end{bmatrix}$$

$$\tilde{\boldsymbol{S}} = \begin{bmatrix}\boldsymbol{S}_a & \boldsymbol{0} \\ \boldsymbol{0} & \boldsymbol{S}_{\beta_{i-1}}\end{bmatrix}$$

where: a tilde is used to mark vectors or matrices that are extended relative to the OE formulation of Eq. 1; the extended state vector, $\tilde{\boldsymbol{z}}$, consists of SST, TCWV and one bias parameter per channel; the prior value of the state vector with respect to SST is the drifting buoy temperature of the match minus 0.17 K, the prior water vapour is the usual prior from NWP, and the three estimated bias parameters from the previous, $(i-1)^{\text{th}}$, retrieval; the extended tangent linear matrix, $\tilde{\boldsymbol{K}}$, consists of partial derivatives of BTs with respect to SST and TCWV, from RTTOV, plus the identity matrix, since the derivative of the corrected simulation of a BT with respect to its own bias parameter is 1; the prior error covariance is block diagonal, the upper-left block corresponding to the error covariance for $\boldsymbol{z}_a$, the lower-right block being the error covariance matrix of the estimated bias parameters (discussed further below); and the bias correction, $\boldsymbol{\beta}_{i-1}$, is applied within the simulation minus observation term.

The bias parameters are forward model parameters whose estimates are improved successively over many retrieval instances. $\boldsymbol{S}_{\beta_{i-1}}$ is initialised as a diagonal matrix assuming small uncertainties (0.01 K for each bias parameter). After retrieval, the posterior error covariance estimate is

$$\boldsymbol{S}_{\tilde{z}_i} = \left(\tilde{\boldsymbol{K}}^{\mathrm{T}}\boldsymbol{S}_\epsilon^{-1}\tilde{\boldsymbol{K}} + \tilde{\boldsymbol{S}}^{-1}\right)^{-1} = \begin{bmatrix}\boldsymbol{A} & \boldsymbol{B} \\ \boldsymbol{C} & \boldsymbol{S}_{\beta_i}\end{bmatrix} \qquad \text{Eq. 7}$$

which is a 5 x 5 matrix. The matrices $\boldsymbol{A}$, $\boldsymbol{B}$ and $\boldsymbol{C}$ are not further used, but the lower-right 3 x 3 block acts as the prior error covariance of the bias parameters for the next retrieval, $\boldsymbol{S}_{\beta_i}$. The main difference of the successive estimation described by these equations from Kalman filtering is the lack of connection between iterations other than via the bias parameters and their error covariance (the iteration index, i, in Eq. 6 is used only for terms that pass some information to the next retrieval). In Kalman filtering, the iterations are typically successive in time and space, and the full retrieved state vector for iteration i acts as an initial estimate for $i+1$. Here, the next retrieval is randomly drawn from the MD and only the bias parameter estimates and their error covariance are relevant: this is why $\tilde{\boldsymbol{S}}$ is block-diagonal, there being no correlation between the errors in the bias parameters and the prior errors in the next, randomly drawn, match.

After a sufficient succession of iterations, the bias parameter estimates stabilise. The average across many stabilised estimates, $\boldsymbol{\beta}$, serves as the parameter set passed to the next step, which is estimation of the simulation-observation error covariance.

5.4. Estimating S-O error covariance

For estimating the error covariance of the simulations relative to observations, we make use of a result from Desroziers et al. (2005; equation 3). Written in the retrieval nomenclature of this paper, the expression is:

$$E[(\boldsymbol{y}-\boldsymbol{F}'(\hat{\boldsymbol{z}}))(\boldsymbol{y}-\boldsymbol{F}'(\boldsymbol{z}_a))^{\mathrm{T}}]=\boldsymbol{S}_\epsilon \qquad \text{Eq. 8}$$

where $\boldsymbol{F}'=\boldsymbol{F}+\boldsymbol{\beta}$. Here, the retrieved vector, $\hat{\boldsymbol{z}}$, consists only of the state variables, SST and TCWV. For the purpose of parameter estimation, the prior SST is again that of the drifting buoy corrected for the skin effect. $E[.]$ signifies expectation. The expression therefore says that the outer product of two terms on average equals the simulation-observation error covariance we seek to estimate. The two terms are the difference between the observations and the simulation for the retrieved state, and the difference between the observations and the simulation for the prior state. Note that a covariance matrix is strictly symmetric, whereas the outer-product inside the expectation operator is not in general symmetric. To reverse Eq. 8 in order to provide an estimate for $\boldsymbol{S}_\epsilon$, three adaptations are made. First, we must estimate the expectation as the average of many instances. (Ideally, we would have many realisations of the same instance, but this is impossible.) Second, since Eq. 8 assumes the bias free case, and biases may not on any given evaluation have been fully removed, the expression should be re-zeroed. Third, we must force the result to be strictly symmetric. Using $\langle . \rangle$ to indicate the arithmetic average over instances, we have:

$$\begin{aligned}\widehat{\boldsymbol{S}}_\epsilon &= \frac{1}{2}\langle \boldsymbol{d}_r^o \boldsymbol{d}_a^{o\mathrm{T}} + \boldsymbol{d}_a^o \boldsymbol{d}_r^{o\mathrm{T}} \rangle \\ \boldsymbol{d}_r^o &= \boldsymbol{y}-\boldsymbol{F}'(\hat{\boldsymbol{z}})-\langle \boldsymbol{y}-\boldsymbol{F}'(\hat{\boldsymbol{z}})\rangle \\ \boldsymbol{d}_a^o &= \boldsymbol{y}-\boldsymbol{F}'(\boldsymbol{z}_a)-\langle \boldsymbol{y}-\boldsymbol{F}'(\boldsymbol{z}_a)\rangle\end{aligned} \qquad \text{Eq. 9}$$

If we have prior reason to expect that $\boldsymbol{S}_\epsilon$ is a function of a quantity we have access to, Eq. 9 can be applied to data stratified with respect to that quantity, to uncover the dependence.

5.5. Estimating the prior error covariance

Desroziers et al. (2005) also derived the equivalent of the following expression (their eq. 2):

$$E[(\boldsymbol{F}'(\hat{\boldsymbol{z}})-\boldsymbol{F}'(\boldsymbol{z}_a))(\boldsymbol{y}-\boldsymbol{F}'(\boldsymbol{z}_a))^{\mathrm{T}}]=\boldsymbol{K}\boldsymbol{S}_a\boldsymbol{K}^{\mathrm{T}} \qquad \text{Eq. 10}$$

Note that, even if $\boldsymbol{S}_a$ were constant (which we have prior reason to doubt with respect to the TCWV error), $\boldsymbol{K}$ is variable between matches. We have an estimate of $\boldsymbol{K}$ from the forward model for each match. While in data assimilation, $\boldsymbol{K}\boldsymbol{S}_a\boldsymbol{K}^{\mathrm{T}}$ is often assessed "in observation space", here we wish to extract an estimate for $\boldsymbol{S}_a$. We wish to use an average of many instances to evaluate the expectation, and to cast the equation in a re-zeroed form that forces a symmetric answer. Combining these requirements, we obtain:

$$\begin{aligned}\widehat{\boldsymbol{S}}_a &= \frac{1}{2}\langle (\boldsymbol{K}^{\mathrm{T}}\boldsymbol{K})^{-1}\boldsymbol{K}^{\mathrm{T}}\left(\boldsymbol{d}_a^r \boldsymbol{d}_a^{o\mathrm{T}} + \boldsymbol{d}_a^o \boldsymbol{d}_a^{r\mathrm{T}}\right)\boldsymbol{K}(\boldsymbol{K}^{\mathrm{T}}\boldsymbol{K})^{-1}\rangle \\ \boldsymbol{d}_a^r &= \boldsymbol{F}'(\hat{\boldsymbol{z}})-\boldsymbol{F}'(\boldsymbol{z}_a)-\langle \boldsymbol{F}'(\hat{\boldsymbol{z}})-\boldsymbol{F}'(\boldsymbol{z}_a)\rangle\end{aligned} \qquad \text{Eq. 11}$$

Again, this can be applied to data stratified with respect to a quantity to uncover the dependence on that quantity, the quantity of relevance here being TCWV. (The SST uncertainty is considered more likely to be constant.)

5.6. Consistency and convergence

A further relationship, from Andersson (2003), can be calculated as a metric of self-consistency. If the error covariance matrices are representative then

$$\langle \widehat{\boldsymbol{S}}_{\epsilon} + \boldsymbol{K}\widehat{\boldsymbol{S}}_{a}\boldsymbol{K}^{\mathrm{T}}\rangle^{-1}\langle \boldsymbol{d}_{a}^{o}\boldsymbol{d}_{a}^{o\,\mathrm{T}}\rangle - \boldsymbol{I} \approx \boldsymbol{0} \qquad \text{Eq. 12}$$

where $\boldsymbol{0}$ is a square matrix of zeros. The element-wise sum of squares of the expression on the left-hand side is a measure of the inconsistency of the error covariance assumptions: as the value decreases, inconsistency decreases and the assumptions are more consistent with the data. This metric can be evaluated once per cycle of estimation (Figure 1) to verify that consistency is improving (i.e., that the inconsistency metric is decreasing).

As a convergence criterion, given the primary aim of SST retrieval in this study, we compared the retrieved SSTs for a given cycle to the retrieved SSTs from the previous cycle. If the retrieved SSTs have changed little, then further cycles serve no practical purpose. this means that the minimum number of cycles of estimation is two. Specifically, we take the estimation process as having converged if the standard deviation of the differences is less than 0.015 K (1.5 cK).

5.7. Decomposing covariance matrices

Numerical values in covariance matrices are relatively difficult to interpret. It is more intuitive to look at the values uncertainty for different terms together with the correlation coefficients of the errors between terms. Results for covariance matrices in this paper are therefore decomposed into constituent parts, as follows:

$$\boldsymbol{S} = \boldsymbol{URU} \qquad \text{Eq. 13}$$

where $\boldsymbol{U}$ is diagonal and holds the uncertainty values, and $\boldsymbol{R}$ contains correlation coefficients (with 1s on the diagonal). The diagonal values of $\boldsymbol{U}$ and the lower-left triangle of $\boldsymbol{R}$ are then presented in tabular form for ease of reading and interpretation. (The first instance is in §Table 2.)

6. Results

6.1. Parameter estimation

The parameter estimates from four estimation cycles are shown in Table 2.

Table 2. Estimated bias and covariance parameters for optimal estimation.

Parameter / units	Applicability		Ini-tial	Cycle 1	Cycle 2	Cycle 3	Cycle 4
Bias / cK	QL = 4	8.7 μm	0	1	2	2	2
		10.8 μm	0	1	1	1	1
		12.0 μm	0	5	5	5	5
	QL = 5	8.7 μm	0	7	8	7	7
		10.8 μm	0	7	8	8	8
		12.0 μm	0	10	11	11	11
S-O uncer-tainty / cK	Near nadir ($s = 1.1$)	8.7 μm	20	23	25	25	25
		10.8 μm	20	12	12	12	12
		12.0 μm	22	10	11	12	13
	Slant path ($s = 2.1$)	8.7 μm	33	28	30	31	32
		10.8 μm	33	19	21	22	23
		12.0 μm	35	23	26	29	31
S-O error correlation	Near nadir ($s = 1.13$)	8.7 μm vs 10.8 μm	0.00	0.32	0.44	0.49	0.51
		10.8 μm vs 12.0 μm	0.00	-0.38	-0.31	-0.21	-0.11
		12.0 μm cs 8.7 μm	0.00	-0.18	0.08	0.19	0.25
	Slant path ($s = 2.08$)	8.7 μm vs 10.8 μm	0.00	0.70	0.78	0.81	0.82
		10.8 μm vs 12.0 μm	0.00	0.48	0.61	0.68	0.72
		12.0 μm vs 8.7 μm	0.00	0.41	0.57	0.62	0.65
Buoy SST uncertainty / cK	Low TCWV ($w = 1.4$ g cm^{-2})		20	23	27	29	31
	High TCWV ($w = 4.0$ g cm^{-2})		20	21	23	23	23
Prior TCWV uncertainty / g cm^{-2}	Low TCWV ($w = 1.4$ g cm^{-2})		0.35	0.27	0.24	0.25	0.21
	High TCWV ($w = 4.0$ g cm^{-2})		0.67	0.36	0.36	0.35	0.35
SST-TCWV error corre-lation	Low TCWV ($w = 1.4$ g cm^{-2})		0.0	-0.13	-0.16	-0.15	-0.15
	High TCWV ($w = 4.0$ g cm^{-2})		0.0	0.04	0.07	0.09	0.11
Inconsistency metric			2.16	0.49	0.19	0.09	0.05
SD of difference in SST from previous cycle / cK			n/a	41	2.4	1.7	1.4

The bias parameters for each channel are estimated using the method described in §5.3, initialised for the first cycle as described in §5.2. The parameter estimates stabilise after ~30,000 iterations in the first

estimation cycle (Figure 3) and change little in subsequent cycles. As expected, given that the operational bias adjustments are already applied, the retrieved bias parameters are small, of order 0.1 K or less. There is a difference between the results by quality level, with the QL = 4 observations being 0.05 K to 0.07 K cooler than the QL = 5 observations. This is consistent with the QL = 4 pixels being more prone to minor amounts of cloud contamination, in line with the intention of the quality flagging algorithm.

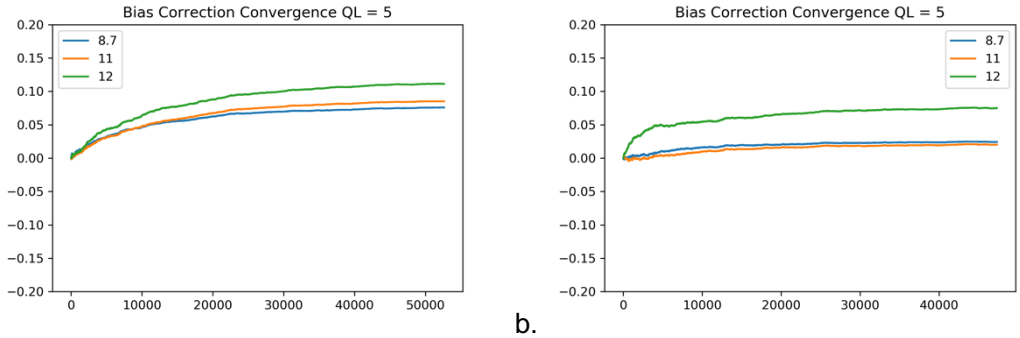

a. b.

Figure 3. Stabilisation of bias parameters from first cycle of estimation for (a.) quality level 5 and (b.) quality level 4 matches.

After the bias estimation in each cycle, new optimal estimation retrievals are made applying those new bias correction estimates per quality level. From these OE results, as described in §5.4, a set of values $\boldsymbol{d}_a^o$ and $\boldsymbol{d}_r^o$ are obtained and used in Eq. 9 to obtain an estimate for the simulation-observation error covariance matrix. Given that some dependence on path is expected, the error covariance matrix is estimated from the data stratified into quartiles of s. The results for the first and fourth quartile are tabulated in Table 2, and the expectation that the uncertainty increases with increasing path (higher satellite zenith angles) is confirmed. Not previously expected is the result that the uncertainty in the 8.7 μm channel is significantly greater than in the 10.8 and 12.0 μm channels, meaning that the addition of the 8.7 μm contains less additional information content with respect to SST than previously thought. Further, the uncertainties for the 10.8 and 12.0 μm channels are less than the initial estimate, which may reflect improvements in forward modelling of those channels, since those initial estimates were inferred (by ad hoc means) in relation to an earlier RTTOV version.

Near nadir, the correlation in error inferred between the 10.8 and 12.0 μm channels is small. This would be consistent with the sensor noise contributing most of the uncertainty in simulation-minus-observation in near-nadir cases. For the quartile of highest satellite zenith angle, the inter-channel correlation is between 0.65 and 0.82, depending on which channel pair is considered. This increase in inferred error correlation cannot be a sensor effect: the noise sources in the instrument doesn't "know" what the satellite zenith angle is. The increase in error correlation is consistent with increasing importance (relative to sensor noise) of forward model uncertainty for more slanted paths through the atmosphere.

RTTOV simulation errors are expected to be correlated between channels, since the same structure of parameterisation is used for different channels. To examine the plausibility of the inferred correlations, we obtained (P. Brunel, pers. comm.) data from simulations used in the training of the RTTOV v11 parameterisations. Differences between RTTOV channel-integrated BTs (i.e., corresponding to the simulations here) and spectrally resolved calculations for the same conditions are, as anticipated, correlated, and the correlations for a path of 2 are comparable to those inferred by the parameter estimation process (Table 2). Moreover, being a difference between simulations, the error correlation for simulations of the real atmosphere may be higher than these correlations of simulation differences. The

parameter estimation results are therefore plausible.

Table 3. Correlation coefficients between RTTOV channel-integrated and spectrally resolved simulations of brightness temperature (RTTOV parameterisation training set).

Path	8.7 μm vs. 10.8 μm	12.0 μm vs 10.8 μm	8.7 μm vs 12.0 μm
1 (0°)	0.30	0.80	0.71
2 (60°)	0.54	0.71	0.79

The uncertainty in the buoy SST is also updated by the estimation procedure. Buoy SST measurement uncertainty is expected to be 0.2 K. The uncertainty relevant here is the uncertainty in using the buoy SST as an estimate of the average skin temperature over a satellite pixel. In this context, the variability in the depth-skin relationship (since we use here just a mean skin effect adjustment) and the point-to-pixel variability both add to the intrinsic measurement uncertainty of the drifting buoy. The prior error covariance matrix is modelled here as a function of total column water vapour, although for the buoy SST uncertainty, no direct dependence is expected. However, for the quartile of lowest TCWV, the parameter estimation process converges on a larger uncertainty estimate, 0.31 K. Since the lower TCWVs all occur towards the limb of the satellite disk, it may be that this really reflects a growth in point-to-pixel variability as the satellite field of view increases. For the other quartiles, the apparent buoy uncertainty is 0.22 K to 0.24 K, in line with expectations. It is not expected that the buoy SST errors should correlate with NWP TCWV, and indeed the inferred correlation coefficients are close to zero.

The initial estimates of uncertainty in TCWV are 25% and 17% at 1.4 and 4.0 g cm^{-2} respectively, and these are markedly greater than the new estimates, which correspond to 15% and 9% respectively. The new estimates are plausible and we regard them as having a more justifiable methodological basis.

Lastly, we note that the inconsistency metric does reduce (consistency improves) on each iteration of the parameter estimation process. The difference between retrieved SSTs using each new set of parameters also decreases each time, and falls below the convergence criterion of 1.5 cK when comparing the results of the third and fourth cycles.

6.2. Impact on OE SST retrieval

To examine the impact of the new OE parameter estimates on retrieved SSTs, the test MD is used, which contains 165574 matches from 2012. Applying parameters estimated for 2011 to 2012 makes the assumption that the sensor biases and noise levels do not change significantly over the course of a year. For a fair test, it is necessary to use a prior SST that is independent of drifting buoys, and so a daily climatological SST is used based on the years 1982 to 2010 inclusive. The climatology is that Merchant et al. (2019), which is the v2 satellite-based dataset from the ESA climate change initiative for SST. SEVIRI is not used in creating this dataset. Being a climatology, inter-annual variability is the dominant source of uncertainty in this prior, and the prior uncertainty is estimated to be 0.85 K for the area within the SEVIRI disk. Zero correlation with NWP TCWV is expected. The prior error covariance matrix is modified accordingly for this test, while all other OE parameters are unchanged, since these are not dependent on what prior SST is used. The results, along with other results for comparison, are shown in Table 4 (as “Tuned OE” results).

Table 4. Impact on validation statistics.

Retrieval	Stra-tum	N	Mean / cK	SD / cK	Median / cK	RSD / cK	$\langle d\hat{x}/dx \rangle$
Climatol-ogy (Prior)	All	165574	-35	81	-28	74	-
Opera-tional	All	165574	-3	50	0	43	-
	QL = 5	87244	1	47	4	40	-
	QL = 4	78330	-9	53	-5	44	-
Initial OE	All	165574	-11	51	-7	43	65%
	QL = 5	87244	-9	48	-5	41	66%
	QL = 4	78330	-14	53	-9	45	64%
Tuned OE	All	165574	-7	50	-3	41	80%
	QL = 5	87244	-6	46	-3	39	81%
	QL = 4	78330	-8	53	-3	44	78%
Tuned OE OSTIA prior	All	165574	-1	44	1	38	80%
	QL = 5	87244	0	42	1	36	81%
	QL = 4	78330	-2	48	1	40	78%

The climatology is in general cooler than the ocean in 2012, reflecting the tendency to warmer SST over time. The root-mean square error in the climatology is 0.85 K and this was used as the prior uncertainty for both the “initial” and “tuned” OE retrievals.

For comparison, the operational retrieval results are first shown. The operational retrieval is based on retrieval coefficients derived by regressing bias-corrected BTs to drifting buoys, plus an additional step of adjustment based on a simulation of the retrieval error (Leborgne, et al, 2011). It therefore combines the empirical basis of regression coefficients with additional information from forward simulation, the latter step providing the extra information that OE also contributes (relative to a purely regression-based retrieval). The results are very good, with a standard deviation relative to buoys of 0.50 K overall (QL 4 and 5 combined).

OE with only the operational bias correction and the initial error covariance assumptions also performs well. This reflects the facts that the operational bias correction addresses most of the observation biases efficiently, and that the error covariance assumptions were based on considerable trial and error. The results are more negatively biased than the operational retrieval, by almost 0.1 K, but otherwise are comparable to the operational results.

The newly tuned OE is marginally less biased (-0.07 K relative to buoys on average) and gives marginally smaller standard deviations of SST than both the operational and initial OE formulation, most of the improvement being from the QL = 5 data. Relative to the initial OE, the retrieval sensitivity is also usefully greater, at around 80%. (The sensitivity quantifies the amount of change in retrieved SST that is obtained per unit change in the true SST. Since the applications of SEVIRI include quantifying the diurnal cycle, it is preferable to have sensitivity close to 100% to ensure the diurnal cycle is well captured It can be easy to improve validation statistics while sacrificing sensitivity (e.g., Petrenko et al., 2014), so the fact that the parameter estimation process has improved the statistics and the sensitivity simultaneously is very positive.

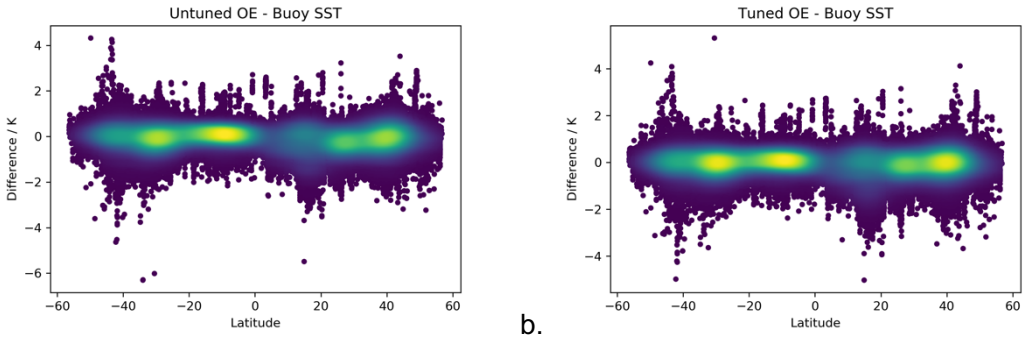

a. b.

Figure 4. Distribution of OE SST minus buoy SST differences against latitude for (a.) untuned and (b.) tuned OE.

Despite not being parameterised in terms of latitude, the tuned OE results show somewhat less latitudinal structure (Figure 4 and §10.3).

Results for one further case are also shown. Operationally, SST retrieval would not typically use a climatology as first guess because more precise prior information is available in the form of SST analysis products that are produced in near real time. OE using OSTIA as a prior SST is shown. So as not to constrain the result too closely, the prior uncertainty is kept the same as for the OE retrievals started from the climatological prior. The improved prior leads to a marked reduction in retrieval errors compared to all the other retrieval formulations. Note that the statistics are likely to be somewhat optimistic because OSTIA assimilates most of the same buoy SSTs as used here for validation.

7. Discussion

The results in Table 4 show that, given the operational bias correction, OE initialised from climatology is comparable to the operational retrieval. The parameter retrieval process leads improved retrievals with less bias, smaller standard deviation when validated on independent data, and improved retrieval sensitivity.

Although real, the gains are fairly modest (because there had already been considerable ad hoc tuning behind the initial formulation).

The study demonstrates other useful results beyond improvements in SST retrieval and opens up several avenues for further work.

First, the study demonstrates an objective method for exploiting the MD that is available operationally in order to address biases of observations relative to simulations. The present bias correction is shown to be efficient, but nonetheless leaves a residual level of bias that degrades the initial OE results, leading to negative bias in excess of 0.1 K. This study shows that a residual bias can be retrieved using the MD as an anchor, which enables OE retrievals that are less biased. The concept of retrieving the bias over many retrievals is a powerful one, and could be exploited to supersede rather than supplement the operational bias correction method (which is somewhat ad hoc).

8. Conclusions and recommendations

1. Simulation-observation bias estimation is crucial to SST retrieval quality from SEVIRI. A method of bias parameter estimation, loosely based on Kalman filtering, has been demonstrated and may offer benefits relative to the currently operational method. It has been demonstrated relative to a in situ MD, but correction of bias relative to other anchors, such as SLSTR, could also be explored. It is recommended that the relevance of the method for bias parameter estimation demonstrated simply here is explored as the focus of a future study.
2. The uncertainty of simulation-observation differences has been estimated for the 8.7, 10.8 and 12.0 μm channels. The results suggest that the uncertainties are greater for the 8.7 μm channel, which may be noisier than previously understood.
3. Significant error correlation is inferred between the SEVIRI window channels, which materially affects multi-channel retrievals and their uncertainties. The error correlations inferred are compatible with the correlations between different simulations related to RTTOV parameterisation. If known, such error correlation information can be directly used in the context of OE. It is recommended that more effort is put into quantifying error correlations in RTTOV simulations, and communicating these to users.
4. The estimate for buoy SST uncertainty is greater at low TCWV values, whereas at other regimes of TCWV it was as expected. It is proposed that this is actually a pixel-size effect at high satellite zenith angles (where the low TCWV values are), but it is recommended that this be investigated.
5. The uncertainty in total column water vapour has been re-estimated and is much less than previously assumed. The new information has a much sounder methodological basis. In the course of OE, TCWV is also retrieved, although not presently used. TCWV retrievals derived using the new uncertainty estimates are thereby put on a more rigorous basis, and their potential usefulness could be further explored.
6. The parameter estimates based on 2011 work well when applied to data from 2012. This suggests that the OE parameters change relatively slowly, which means they could be operationally applied and routinely updated on a feasible cycle (e.g., monthly incremental updates).
7. Various aspects have not been addressed in this short study. It is recommended that these be pursued to build on the work:
    a. The error covariances have been derived on strata of variables already known to be useful (atmospheric path and prior TCWV). Now that a systematic means of estimating error covariances is available, it is recommended that alternatives be explored that may enable them to be better optimised. For example:
        i. the simulation-observation error covariances almost certainly should be increased under desert-dust conditions
        ii. the water vapour path may better predict RTTOV errors
    b. Only a global bias correction per quality level (on top of the operational bias correction) is estimated here. It is very likely that seasonal-regional residual biases are present that would be well estimated using the method on those, or perhaps even shorter, scales. This could unlock significant progress in reducing SST uncertainty.

9. References

Andersson, E (2003). Modelling of innovation statistics'. Pp.153–164 of Proceedings of Workshop on recent developments in data assimilation foratmosphere and ocean, ECMWF, Reading, UK

Bormann, N., M. Bonavita, R. Dragani, R. Eresmaa, M. Matricardi, and A. McNally, 2016:Enhancing the impact of IASI observations through an updated observation-error covariance matrix. Quarterly Journal of the Royal Meteorological Society,142 (697), 1767–1780, doi:56310.1002/qj.2774

Campbell, W. F., E. A. Satterfield, B. Ruston, and N. L. Baker, 2017: Accounting for correlated observation error in a dual-formulation 4d variational data assimilation system. Monthly Weather Review,145 (3), 1019–1032, doi:10.1175/MWR-D-16-0240.1.

Cordoba, M., S. Dance, G. Kelly, N. Nichols, and J. Waller, 2017: Diagnosing atmospheric motion vector observation errors for an operational high resolution data assimilation system. Quarterly Journal of the Royal Meteorological Society,143 (702), 333–341, doi:10.1002/qj.2925

Dee, D. P. (2005), Bias and data assimilation. Q.J.R. Meteorol. Soc., 131: 3323-3343. doi:10.1256/qj.05.137

Desroziers, G, L Berre, B Chapnik and P Poli (2005). Diagnosis of observation, background and analysis-error statistics in observation space. Q. J. Roy. Meteorol. Soc. doi: 10.1256/qj.05.108, 2005

Koner, P. K., A. Harris and E. Maturi (2015) A Physical Deterministic Inverse Method for Operational Satellite Remote Sensing: An Application for Sea Surface Temperature Retrievals. IEEE Trans. Geosci. Rem. Sens. 53(11) 10.1109/TGRS.2015.2424219

Lean, K. and Saunders, R. (2013), Validation of the ATSR Re-processing for Climate (ARC) dataset using data from drifting buoys and a three-way error analysis. Amer. Met. Soc. J. Climate vol 26, issue 13, pp.4758-4772

Le Borgne, P., Roquet, H. and Merchant, C. J. (2011) Estimation of sea surface temperature from the Spinning Enhanced Visible and Infra Red Imager, improved using numerical weather prediction. Remote Sensing of Environment, 115 (1). pp. 55-65. ISSN 0034-4257 doi: https://doi.org/10.1016/j.rse.2010.08.004

Merchant, C. J., Le Borgne, P., Marsouin, A. and Roquet, H. (2008) Optimal estimation of sea surface temperature from split-window observations. Remote Sensing of Environment, 112 (5). pp. 2469-2484. ISSN 0034-4257 doi: https://doi.org/10.1016/j.rse.2007.11.011

Merchant, C. J., Le Borgne, P., Roquet, H. and Marsouin, A. (2009) Sea surface temperature from a geostationary satellite by optimal estimation. Remote Sensing of Environment, 113 (2). pp. 445-457. ISSN 0034-4257 doi: https://doi.org/10.1016/j.rse.2008.10.012

Merchant, C. J., Le Borgne, P., Roquet, H. and Legendre, G. (2013) Extended optimal estimation techniques for sea surface temperature from the Spinning Enhanced Visible and Infra-Red Imager (SEVIRI). Remote Sensing of Environment, 131. pp. 287-297. ISSN 0034-4257 doi: https://doi.org/10.1016/j.rse.2012.12.019

Minnett, P. J., M. Smith and B. Ward, 2011. Measurements of the oceanic thermal skin effect. Deep Sea Research Part II: Topical Studies in OceanographyVolume 58, Issue 6, 15 March 2011, Pages 861-868,

DOI: 10.1016/j.dsr2.2010.10.024

Petrenko, B., A. Ignatov, Y. Kihai, J. Stroup, and P. Dash (2014), Evaluation and selection of SST regression algorithms for JPSS VIIRS, J. Geophys. Res. Atmos., 119, 4580–4599, doi:10.1002/2013JD020637.

Stewart, L. M., S. L. Dance, N. K. Nichols, J. R. Eyre, and J. Cameron, 2014: Estimating inter-channel observation-error correlations for IASI radiance data in the Met Office system.Quar-641terly Journal of the Royal Meteorological Society,140 (681), 1236–1244, doi:10.1002/qj.2211

Waller, J. A., D. Simonin, S. L. Dance, N. K. Nichols, and S. P. Ballard, 2016c: Diagnosing observation error correlations for Doppler radar radial winds in the Met Office UKV model using observation-minus-background and observation-minus-analysis statistics. Monthly Weather675Review,144 (10), 3533–3551, doi:10.1175/MWR-D-15-0340.1

Waller, J. A., S. P. Ballard, S. L. Dance, G. Kelly, N. K. Nichols, and D. Simonin, 2016a: Diagnosing horizontal and inter-channel observation error correlations for SEVIRI observations using observation-minus-background and observation-minus-analysis statistics. Remote Sensing,8 (7), 581, doi:10.3390/rs8070581

Weston, P. P., W. Bell, and J. R. Eyre, 2014: Accounting for correlated error in the assimilation of high-resolution sounder data.Quarterly Journal of the Royal Meteorological Society,140 (685),6842420–2429, doi:10.1002/qj.2306.

Wong, E. W., & Minnett, P. J. (2018). The response of the ocean thermal skin layer to variations in incident infrared radiation. Journal of Geophysical Research: Oceans, 123, 2475-2493. https://doi.org/10.1002/2017JC013351

10. Appendices

10.1. Based on 2011 MD

The values of inferred parameters for all quartiles are tabulated below for reference. The values have been saved in netcdf files and provided to the OSI-SAF.

```
netcdf parameter_estimates_2011_4 {
dimensions:
    nchan = 3 ;
    ntcwv = 4 ;
    npath = 4 ;
    nzvar = 2 ;
    nql = 2 ;
variables:
    float chan(nchan) ;
        chan:units = "micrometres" ;
        chan:long_name = "channel central wavelength" ;
        chan:standard_name = "wavelength" ;
    float tcwv(ntcwv) ;
        tcwv:units = "g / cm^2" ;
        tcwv:long_name = "reference values of total column water vapour
for covariance model" ;
        tcwv:standard_name = "tcwv" ;
    float path(npath) ;
        path:units = "g / cm^2" ;
        path:long_name = "reference values of secant of satellite zenith
angle" ;
        path:standard_name = "sectheta" ;
    float Sa(nzvar, nzvar, ntcwv) ;
        Sa:units = "mixed" ;
        Sa:long_name = "prior error covariance parameters by tcwv" ;
        Sa:comment = "2 x 2 x 4: [[usst^2], [usst*utcw]], [[usst*utcw],
[utcw^2]] x tcwv" ;
        Sa:standard_name = "S_a" ;
    float Se(nchan, nchan, npath) ;
        Se:units = "K^2" ;
        Se:long_name = "sim-obs error covariance parameters by path" ;
        Se:standard_name = "S_e" ;
        Se:comment = "3 x 2 = channels x quality level [QL4, QL5]" ;
    float beta(nchan, nql) ;
        beta:units = "K" ;
        beta:long_name = "bias correction parameters" ;
        beta:standard_name = "bc" ;
data:

 chan = 8.7, 10.8, 12 ;
```

```
 tcwv = 1.418967, 2.099057, 2.834442, 3.970806 ;

 path = 1.130943, 1.41805, 1.680825, 2.087907 ;

 Sa =
  0.09504894, 0.05061651, 0.06532113, 0.07487753,
  -0.00974864, -0.01551126, 0.0005782479, 0.01040876,
  -0.009748637, -0.01551126, 0.0005782468, 0.01040876,
  0.04598793, 0.06651784, 0.09481356, 0.1247599 ;

 Se =
  0.06448417, 0.03926921, 0.04875163, 0.1012976,
  0.01517007, 0.01370855, 0.02680052, 0.06088078,
  0.00799631, 0.0143879, 0.03003672, 0.06407324,
  0.01517007, 0.01370855, 0.02680052, 0.06088078,
  0.01398011, 0.01130527, 0.02314225, 0.05495903,
  -0.001703438, 0.003974373, 0.01991108, 0.05204362,
  0.00799631, 0.0143879, 0.03003672, 0.06407324,
  -0.001703438, 0.003974373, 0.01991108, 0.05204362,
  0.0162547, 0.02864375, 0.05505618, 0.09563842 ;

 beta =
  0.01846741, 0.07460082,
  0.01021159, 0.08039254,
  0.04914828, 0.1118343 ;
}
```

10.2. Based on 2012 MD

The values of inferred parameters for all quartiles are tabulated below for reference. The values have been saved in netcdf files and provided to the OSI-SAF.

```
netcdf parameter_estimates_2012_4 {
dimensions:
    nchan = 3 ;
    ntcwv = 4 ;
    npath = 4 ;
    nzvar = 2 ;
    nql = 2 ;
variables:
    float chan(nchan) ;
        chan:units = "micrometres" ;
        chan:long_name = "channel central wavelength" ;
        chan:standard_name = "wavelength" ;
    float tcwv(ntcwv) ;
        tcwv:units = "g / cm^2" ;
        tcwv:long_name = "reference values of total column water vapour
for covariance model" ;
        tcwv:standard_name = "tcwv" ;
```

```
    float path(npath) ;
        path:units = "g / cm^2" ;
        path:long_name = "reference values of secant of satellite zenith
angle" ;
        path:standard_name = "sectheta" ;
    float Sa(nzvar, nzvar, ntcwv) ;
        Sa:units = "mixed" ;
        Sa:long_name = "prior error covariance parameters by tcwv" ;
        Sa:comment = "2 x 2 x 4: [[usst^2], [usst*utcw]], [[usst*utcw],
[utcw^2]] x tcwv" ;
        Sa:standard_name = "S_a" ;
    float Se(nchan, nchan, npath) ;
        Se:units = "K^2" ;
        Se:long_name = "sim-obs error covariance parameters by path" ;
        Se:standard_name = "S_e" ;
        Se:comment = "3 x 2 = channels x quality level [QL4, QL5]" ;
    float beta(nchan, nql) ;
        beta:units = "K" ;
        beta:long_name = "bias correction parameters" ;
        beta:standard_name = "bc" ;
data:

 chan = 8.7, 10.8, 12 ;

 tcwv = 1.431208, 2.105799, 2.736929, 3.776994 ;

 path = 1.13312, 1.41706, 1.60308, 2.011619 ;

 Sa =
  0.08361942, 0.05516465, 0.05696054, 0.06125894,
  -0.01075144, -0.02143178, -0.01739152, -0.003751766,
  -0.01075149, -0.02143179, -0.01739152, -0.003751766,
  0.05654944, 0.07301553, 0.08530219, 0.1154286 ;

 Se =
  0.03990133, 0.03364344, 0.0401932, 0.06417356,
  0.02176738, 0.01389279, 0.0195967, 0.02921116,
  0.00973857, 0.01560902, 0.02333472, 0.03751936,
  0.02176738, 0.01389279, 0.0195967, 0.02921116,
  0.01971504, 0.01144957, 0.01818538, 0.02649216,
  -0.001346814, 0.005051419, 0.01486389, 0.02982025,
  0.00973857, 0.01560902, 0.02333472, 0.03751936,
  -0.001346814, 0.005051419, 0.01486389, 0.02982025,
  0.01767958, 0.04090315, 0.0560001, 0.08284944 ;

 beta =
  0.02510169, 0.07790193,
  0.02096556, 0.0863958,
  0.06765884, 0.1096381 ;
}
```

10.3. OE validation statistics stratified by latitude

Summary statistics of Tuned retrieval - Buoy / K, stratified by: Latitude

N	Mean	SD	Median	RSD / K
Stratum:	-50 to -30			
30932	-0.047	0.495	-0.015	0.408
Stratum:	-30 to -10			
35171	0.002	0.393	0.029	0.347
Stratum:	-10 to 10			
23242	-0.036	0.435	-0.002	0.362
Stratum:	10 to 30			
34956	-0.213	0.595	-0.138	0.498
Stratum:	30 to 50			
37994	-0.044	0.500	-0.030	0.441

Summary statistics of Untuned retrieval - Buoy / K, stratified by: Latitude

N	Mean	SD	Median	RSD / K
Stratum:	-50 to -30			
30932	-0.081	0.522	-0.046	0.429
Stratum:	-30 to -10			
35171	-0.003	0.389	0.030	0.340
Stratum:	-10 to 10			
23242	-0.052	0.421	-0.008	0.341
Stratum:	10 to 30			
34956	-0.302	0.579	-0.252	0.513
Stratum:	30 to 50			
37994	-0.093	0.516	-0.084	0.465